

Generation and Evaluation of Gold-binding Peptide Fused Protein A

Thuy-Dung Doan-Tran^{1,3,4}, Thanh-Tan Nguyen^{1,2,3,4}, and Hieu Tran-Van^{1,2,3,4,*}

¹Department of Molecular and Environmental Biotechnology, Faculty of Biology and Biotechnology, University of Science Ho Chi Minh City, Vietnam; ²Laboratory of Biosensors, Faculty of Biology and Biotechnology, University of Science Ho Chi Minh City, Vietnam;

³Laboratory of Molecular Biotechnology, University of Science, Ho Chi Minh City, Vietnam; ⁴Vietnam National University, Ho Chi Minh City, Vietnam

Received: December 31, 2022; Revised: March 9, 2023; Accepted: April 4 2023

Abstract

Immobilizing antibodies onto the surface of gold nanoparticles (AuNPs) in an oriented manner is essential to achieve high sensitivity and detection limits in immunoassays and biosensors. In this research, the two-domain protein proAx1-Au-binding was generated as the result of the fusion between staphylococcal protein A and a gold-binding peptide (GBP). This novel protein allows the fragment antigen-binding (Fab) region of captured antibodies to be exposed while binding stably to the gold surface. In this present study, we successfully constructed the recombinant pET22b-proAx1-Au-binding plasmid. The expression of proAx1-Au-binding was induced by Isopropyl β-D-1-thiogalactopyranoside (IPTG) and then confirmed by Tricine-SDS-PAGE and Western Blot. The gold-binding ability of this novel protein was evaluated and the result showed that proAx1-Au-binding had a higher affinity for AuNPs than protein A alone, thereby enhancing antibody immobilization onto AuNPs. This study laid the groundwork for facilitating the preparation of any target-specific antibody-AuNPs.

Keywords: antibody immobilization, gold nanoparticle, gold-binding peptide, immunoassay, protein A

1. Introduction

Gold nanoparticles (AuNPs) have been gaining tremendous attraction in recent years for their potential applications in various fields, especially in biomedicine. This is due to their advantageous size as well as their interesting physical, chemical, and optical properties (Dreaden *et al.*, 2012). The size of AuNPs is in the nanoscale, which is 1-100 nm (Bakshi *et al.*, 2014). Despite their small size, they have a high surface-to-volume ratio which allows them to be conjugated with a wide range of biomolecules (Akbarzadeh Khiavi *et al.*, 2019; Bhumkar *et al.*, 2007; Deka *et al.*, 2017; Kumari *et al.*, 2020; Lin *et al.*, 2021; Rahme *et al.*, 2019; Thomas and Klibanov, 2003). This leads to the development of novel complexes which possess characteristics of both AuNPs and their conjugating partners. Among various types of biomolecules, proteins with diverse structural and functional properties are the most focused, especially antibodies since gold nanoparticle-antibody (AuNP-Ab) conjugates are promising for many diagnostic applications such as biosensing, immunoassay, etc. (Lin *et al.*, 2021)

Two main strategies for conjugating antibodies to AuNPs are non-covalent mode (based on hydrophobic and ion interaction) and covalent mode (based on EDC/NHS reactions, thiol derivatives, and linkers) (Jazayeri *et al.*, 2016). While being relatively simple, the non-covalent method has major weaknesses including weak binding and random orientation of antibodies on particles' surfaces,

reducing immunoassay sensitivity (Saha *et al.*, 2014). Conversely, the covalent mode helps to achieve strong and oriented immobilization. However, this method is labor-intensive and involves chemical modification of antibodies, which can potentially affect the structure and function of those molecules (Katz and Willner, 2004).

The new approach to immobilizing antibodies to AuNPs' surface utilizing gold binding peptides (GBPs) could overcome the limitation of existing methods. These GBPs have a natural affinity with gold material; therefore, they can act as linkers to connect desired molecules with AuNPs. With a high level of modularity in molecular design, GBPs could be fused with different biomolecules through gene engineering to become bi-functional linkers that display both gold-binding qualities as well as characteristics of the fusion partner (Lee *et al.*, 2021; Park *et al.*, 2006). While GBPs can adsorb onto the gold surface easily, they do not bind antibodies; hence, the peptide and another molecule with a natural affinity for antibodies need to be fused. Protein A, originally found in *Staphylococcus aureus*, is probably the most ideal fusion partner in this case since it is capable of binding to the fragment crystallizable (Fc) region of immunoglobulins, especially IgG, from a large number of species (Moks *et al.*, 1986). This property allows the Fab region of antibodies to point outward increasing interaction with antigens. The AuNP-Ab complex conjugated via GBP-protein A fusion protein is expected to be stable, highly interactive with antigens, and therefore considerably

* Corresponding author. e-mail: tvhieu@hcmus.edu.vn.

improve the limit of detection as well as the sensitivity of biosensors and bioassays.

There were previous studies that have conjugated antibodies to AuNPs using protein A-GBP fusion proteins. However, oftentimes the whole protein A was used to generate the fusion protein (Koet *et al.*, 2009). Although protein A consists of five homologous domains and each domain is able to bind IgGs, previous studies showed that each protein A can only bind with approximately two to three IgG molecules (Janset *et al.*, 2009). This means that each fusion protein of gold-binding peptides and protein A can only bind up to three IgG molecules. In this study, a protein A-GBP fusion protein was generated by fusing GBPs with the domain Eof protein A, which has the highest affinity for the Fc region as well as the second-lowest affinity for the Fab region of antibodies, making it the ideal fusion partner for generating the fusion protein (Jansson *et al.*, 1998). This novel fusion protein is expected to be smaller in size while having a strong affinity for antibodies compared to previous protein A-GBP fusion proteins. Our study aims to immobilize antibodies onto AuNPs in an oriented manner using this novel fusion protein (Fig. 1). The gold-binding capability of this fusion protein was evaluated. Antibody immobilization using this fusion protein was also carried out and compared with other conventional strategies.

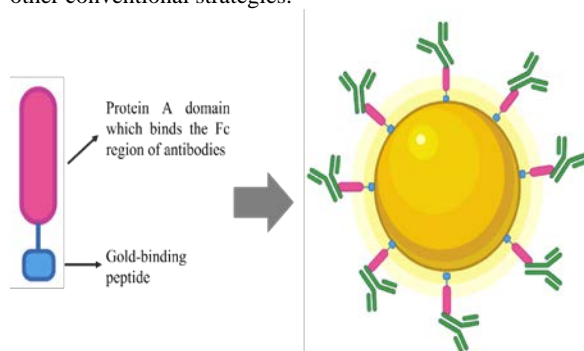


Figure 1. Schematic of immobilization of antibodies onto AuNPs using protein A-GBP fusion protein.

2. Materials and Methods

2.1. Reagents and equipment

Reagents and equipment are listed: proAx1-Au-binding coding template G-block and primers (PHUSA BioChem, Vietnam); restriction enzymes, T4 DNA ligase, and buffers (Thermo Fisher Scientific, USA); MyTaq Red Mix (2X) (Bioline, UK); EZ-10 Spin Column DNA Minipreps Kit (Biobasic, Canada); PCR P25 instrument (PHUSA BioChem, Vietnam); ENDURO™ Gel XL Electrophoresis System (Labnet International); Mini-PROTEAN Electrophoresis System (BIO-RAD, USA); ThermoBioMate 3 Spectrophotometer (Thermo Fisher Scientific, USA); Fluorescence microscope (Nikon, Japan); Horseradish peroxidase (HRP)-conjugated 6*His, His-Tag Monoclonal antibody (ProteinTech, USA); DCNovations Colloidal Gold Conjugation Kit (DCN Dx, USA); GFP-Fc protein; chemicals (Merck, USA), otherwise stated.

2.2. Strains and plasmids

The *E. coli* strain DH5 α was used as a host for the manipulation of recombinant DNA. The *E. coli* strain BL21(DE3) was used for recombinant protein expression. The *E. coli* strain BL21(DE3) carrying pET22b-*proAx1* plasmids was used to express the recombinant protein proAx1 (Tran-Nguyen *et al.*, 2021). The pET22b plasmid used to construct the proAx1-Au-binding expression vector is under the control of T7 promoter and carries an ampicillin resistance gene for screening of transformants and a His-tag sequence (Novagen).

2.3. Construction of pET22b-*proAx1*-Au-binding plasmid

The Au-binding peptide HGKTQATSGTIQS was used in this study (Verde *et al.*, 2009). The DNA coding sequence of the domain E of staphylococcal protein A was obtained from NCBI (GenBank: X61307.1). The DNA coding sequences of domain E and the GBP were fused and optimized for later expressing steps in *E. coli*. The complete *E. coli* optimized, coding region of the *proAx1*-Au-binding gene, was obtained from the G-block template (PhuSa Biochem, Vietnam) by polymerase chain reaction (PCR) with gene-specific primers containing a restriction site of *Nde*I at 5' end and a restriction site of *Hind*III at 3' end. All designed primers are listed in Table 1. The PCR reaction (50 μ l total volume) composed of 25 μ l of MyTaq Red Mix, 1 μ l of protein-coding templates (approximately 1000 ng), and 2 μ l of each primer (10 pmol/ml). The PCR amplification process was performed under the following conditions: an initial denaturation step at 95°C for 3 min; followed by 35 cycles of 95°C for 15 sec, 55°C for 15 sec, 72°C for 30 sec, and a final extension step at 72°C for 6 min. The size of the PCR product was analyzed on agarose gel electrophoresis (1.5%).

The digestion of the pET22b plasmid and the *proAx1*-Au-binding gene with *Hind*III/*Nde*I restriction enzymes was simultaneously carried out in a single reaction for 4 hr for complete digestion (Le-Dao *et al.*, 2022; Mohammad and Soukkarieh, 2022). Digested products were ligated using T4 DNA ligase, then transformed into competent *E. coli* DH5 α cells by heat shock method for the construction of the pET22b-*proAx1*-Au-binding plasmid. Five recombinant clones that grew on LB agar plates containing 100 μ g/ml ampicillin (LB-Amp100) were selected and tested by colony PCR with the same procedure mentioned above to confirm the insertion of the *proAx1*-Au-binding gene into pET22b plasmids.

Table 1 Primer sequences used in this study.

Primer	Sequence
216F-Nde	<u>C</u> ATATGGACAACAAATTCACAAAGAAC
418R-HindIII	AAGCTT <u>G</u> CTCTGAATGGTGCCGCTGGTCG
T7 pro	CGAAATTAATACGACTCACTATAGG
T7 ter	GGTTATGCTAGTTATTGCTCAGCG

Underlined letters indicate the restriction enzyme.

2.4. Expression of the recombinant *proAx1*-Au-binding protein

The recombinant pET22b-*proAx1*-Au-binding plasmid was cloned in *E. coli* BL21(DE3) with the same procedure. The production of proAx1-Au-binding was induced using IPTG (final concentration 0.5 mM) at 37°C for 4 hr. Transformed *E. coli* BL21(DE3) cells bearing the pET22b

plasmid were similarly induced to serve as the control sample. The induced *E. coli* BL21(DE3) cells were lysed in 20 mM PBS buffer (3.8 mM NaH₂PO₄, 16.2 mM Na₂HPO₄, pH 7.4) by sonication (30%, 3 min) to extract total protein and then centrifuged at 13,000 rpm/min for 20 min to obtain supernatant containing soluble proteins and insoluble cell pellets.

2.5. Protein expression analysis with SDS-PAGE and Western Blot

The analysis of Au-binding-proAx1 expression was carried out simultaneously with proAx1 - one of the five homologous domains of staphylococcal protein A - expressed with the same procedure mentioned above. Sample buffer (0.375 M Tris (pH 6.8), SDS 12%, Glycerol 60%, 0.6M DTT, Bromophenol Blue 0.06%, dH₂O) was added to protein samples and heated at 100 °C for 15 min. before being analyzed with Tricine-SDS-PAGE.

Cloning in expression vector pET22b allowed recombinant proteins to be expressed as His-tagged proteins, which could be detected by Western blotting using His-tag antibodies. Protein samples were subjected to Tricine-SDS-PAGE on a 20% gel, after which the unstained gel was transferred to the nitrocellulose membrane and probed with HRP-conjugated His-tag antibodies at dilution of 1:50,000.

2.6. Evaluation of the gold-binding ability

2.6.1. Preparation of AuNPs

Before immobilization, AuNPs were cleaned using 10 mM MES buffer and 10 mM acetate buffer (5.499 mM acetic acid, 4.501 mM sodium acetate, pH 4.5). The colloidal gold solution was first centrifuged at 13,000 rpm/min for 10 min and the pellet of AuNPs was then resuspended in 10 mM MES buffer. The AuNPs were subsequently centrifuged/resuspended one more time before changing into 10 mM acetate buffer (pH 4.5). Similar centrifugation/resuspension cycles were performed with 10 mM acetate buffer (pH 4.5).

2.6.2. Immobilization of proAx1 and proAx1-Au-binding onto AuNPs

The total protein extract from cultured cells expressing proAx1 and proAx1-Au-binding was obtained by lysing cells in 10 mM acetate buffer (pH 4.5). The protein bands of proAx1 and proAx1-Au-binding were quantified based on the result of Tricine-SDS-PAGE with Coomassie staining using ImageJ. The total protein extracts of proAx1 and proAx1-Au-binding were analyzed by Bradford assay to quantify the total protein concentration and then adjusted to achieve an equal molecular amount of proAx1 and proAx1-Au-binding before being incubated with the same amount of prepared AuNPs. The incubation was carried out for 1 hr at 4°C. Excess proteins were removed by centrifugation at 13,000 rpm/min for 10 min. After centrifugation, the supernatant was collected and the pellet was resuspended in 10 mM acetate buffer (pH 4.5). To further wash weakly bound proteins from AuNPs, the centrifugation/resuspension cycle mentioned above was repeated three times. After the final wash, the AuNP-protein precipitates were boiled for 10 min at 100°C in sample buffer to release the protein from the AuNPs. The immobilization of proteins onto AuNPs was then evaluated by Tricine-SDS-PAGE with silver staining.

2.7. Evaluation of the antibody-capturing ability

To evaluate the antibody-capturing ability of the AuNP-protein conjugates, GFP-Fc protein was used in place of normal antibodies since GFP-Fc proteins contain the Fc domain to which protein A bound specifically and the GFP domain which allows fluorescence visualization (Al-Homsi *et al.*, 2012; Nguyen *et al.*, 2021). The final AuNP-protein conjugates obtained after immobilizing proteins onto the AuNPs and washing, as well as AuNPs alone, were incubated with GFP-Fc proteins for 1 hr at 4°C in 10 mM acetate buffer (pH 4.5). After incubation, the same centrifugation/resuspension cycles used in the gold-immobilization step were performed to remove excess and weakly-bound GFP-Fc. The final AuNP-protein-GFP-Fc conjugates were analyzed using fluorescence microscopy. The fluorescence signal of each sample was quantified using ImageJ, function Measure. The minimum threshold was set so that the raw signal of unconjugated AuNPs would not contribute to the signal obtained from the samples which were conjugated with GFP-Fc. The particles with an area above 120,000 square pixels which was significantly bigger compared to the average size of most particles in the samples, hence they were treated as unwanted impurities and excluded from the signal quantification. T-tests were then used to determine whether there was any statistical difference between the fluorescence signal obtained from each sample.

3. Result

3.1. Cloning of the proAx1-Au-binding gene

The *proAx1-Au-binding* gene was successfully amplified by PCR using gene-specific primers. A band of approximately 246 bp, which was the size of the *proAx1-Au-binding* gene, could be observed from the electropherogram (Fig.2A, lane 2). Linearization of the pET22b plasmid was achieved using *NdeI/HindIII* restriction enzymes. The digested product gave a single linear band of approximately 5,493 bp (Fig.2B, lane 4). The *proAx1-Au-binding* gene was successfully cloned into pET22b plasmids in a correct orientation. The result of colony PCR with 416F-NdeI/T7 terprimers showed a band of approximately 400 bp from three out of five screened transformants, which was the expected size of the PCR product (Fig.2C, lane 3, 5, 6).

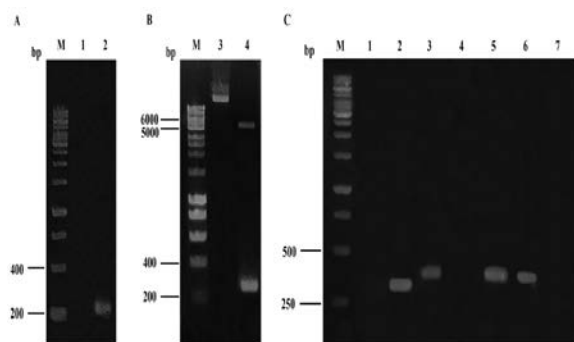


Figure 2. Construction of pET22b-*proAx1-Au-binding* plasmid. (A) PCR amplification of *proAx1-Au-binding*. M, DNA ladder; 1, negative control; 2, *proAx1-Au-binding* gene. (B) *proAx1-Au-binding* gene and pET22b plasmid were digested with *NdeI/HindIII* restriction enzymes. M, ladder; 3, plasmid pET22b; 4, digested products. (C) Screening of transformants carrying pET22b-*proAx1-Au-binding*. M, DNA ladder; 1, negative control; 2, PCR amplification of pET22b plasmids with T7 pro/T7 ter; 3-7, colony PCR of transformants with 416F-Nde/T7 ter.

3.2. Expression of *proAx1-Au-binding*

The *proAx1-Au-binding* and *proAx1* proteins were expressed in *E. coli* BL21(DE3). Bacterial lysate of *E. coli* BL21(DE3) containing pET22b-*proAx1-Au-binding* plasmid after induction with IPTG (final concentration 0.5 mM) at 37°C for 4 hr revealed an over-expressed protein band of approximately 8.9 kDa (Fig.3A, lane 3, 4), which was the predicted size of *proAx1-Au-binding* and higher than the expression band of *proAx1* (approximately 6 kDa) (Fig.3A, lane 2). There was no similar over-expressed band detected in the control lane (Fig.3A, lane 1). Both *proAx1* and *proAx1-Au-binding* were detected in the Western blot experiment employing His-tag antibodies. The result showed corresponding signals to the suspected bands in Tricine-SDS-PAGE (Fig.3B). This further confirmed that *proAx1* and *proAx1-Au-binding* were successfully expressed. As for protein solubility, *proAx1-Au-binding* was mainly expressed in soluble form as expected (Fig.3A-B, lane 4), while *proAx1* was already confirmed to be expressed in soluble form with the same expression condition as previously reported (Tran-Nguyen *et al.*, 2021).

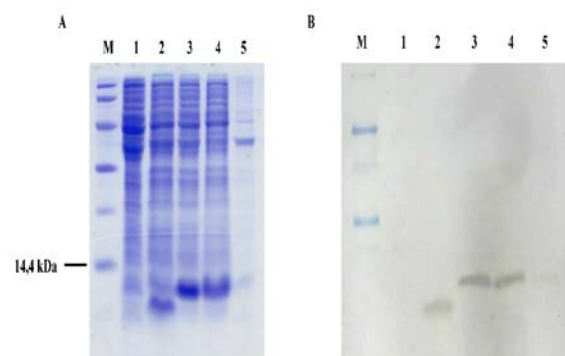


Figure 3. Protein expression analysis of *proAx1* and *proAx1-Au-binding*. (A) SDS-PAGE; (B) Western Blot. M, protein molecular weight ladder; 1: total cellular protein expressed in *E. coli* BL21(DE3) carrying pET22b as a control; 2, total cellular protein of *proAx1*; 3-5, total cellular protein, soluble fraction, insoluble fraction of *proAx1-Au-binding*.

3.3. Immobilization of proteins onto the surface of AuNPs

The immobilization of *proAx1* and *proAx1-Au-binding* onto the surface of AuNPs was facilitated by incubating the mixture of proteins and AuNPs in 10 mM acetate buffer of pH 4.5 at 4°C followed by several washing cycles of centrifugation and resuspension. The supernatant samples of each step were collected to be analyzed by Tricine-SDS-PAGE with silver staining. The result showed that the number of proteins in the mixture surpassed the binding capacity of AuNPs. Thus, unbound proteins remained in the supernatant after centrifugation (Fig. 4, lane 2, 5). The precipitate lanes revealed a major protein band of *proAx1-Au-binding* while no protein band of *proAx1* was observed, which indicated that there was little to no *proAx1* in the final AuNP-protein complex (Fig.4, lane 3, 9). This proved that the binding of *proAx1* to AuNPs was not stable while *proAx1-Au-binding*, which was the fusion of protein A and GBP, was still bound strongly to AuNPs even after being challenged by several washing steps. The result indicated that *proAx1-Au-*

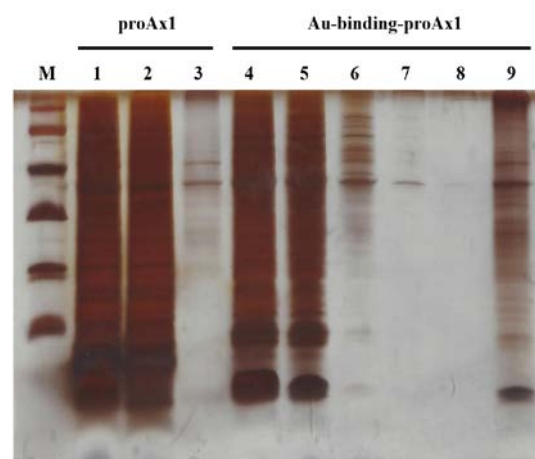


Figure 4. Immobilizing of *proAx1* and *proAx1-Au-binding* onto AuNPs. M, ladder; 1, 4, total protein; 2, 5, supernatant obtained after incubation; 3, 9, final precipitate; 6-8, supernatant of three washing cycles.

3.4. Evaluation of antibodies immobilized onto AuNPs

Two strategies of immobilizing antibodies onto gold surfaces via *proAx1* and *proAx1-Au-binding* were evaluated. After the final wash in the gold-binding assay, the AuNP-protein conjugates were incubated with GFP-Fc and then washed in 10 mM acetate buffer (pH 4.5). The final conjugates obtained were analyzed with fluorescence spectroscopy and ImageJ (Fig. 5A). The fluorescent signal quantification result showed that the immobilization via *proAx1-Au-binding* strategy gave the highest signal of $48,078,802.67 \pm 10,842,323.01$, which indicated the successful capture of GFP-Fc. Meanwhile, the immobilization via *proAx1* strategy showed much less signal of $28,661,414.33 \pm 5,162,967.87$, since little to no *proAx1* was presented in the initial conjugates, as demonstrated in the silver staining analysis. The direct absorption strategy giving the lowest signal of $15,547,923.67 \pm 2,640,668.05$ also proved that most of the

uncaptured GFP-Fc remained in the supernatant after centrifugation, so the fluorescent signal was obtained mainly owing to the binding of GFP-Fc to proteins. The t-test results (all two-tailed) indicated that there was a statistical difference between each pair of samples with p-values < 0.05 (Fig. 5B). These results demonstrated that the strategy to immobilize antibodies onto AuNPs via the two-domain protein proAx1-Au-binding was much more effective compared to immobilizing via protein A or direct absorption.

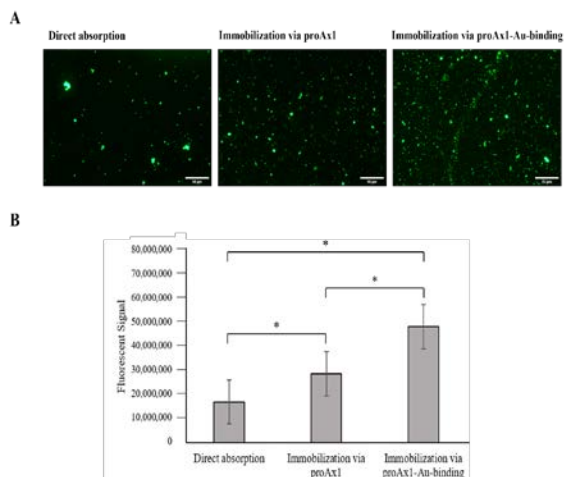


Figure 5. Visualization of GFP-Fc immobilization by fluorescence microscope (A) (x20 magnification; scale-bar: 50 μ m) and the comparison of the fluorescent signal of GFP-Fc immobilizing strategies (B). Data represent three replications and are expressed as mean \pm standard deviation. *p < 0.05.

4. Discussion

The novel fusion protein proAx1-Au-binding has a gold-binding domain and a protein A domain which captures the Fc region of antibodies and, therefore, allows the Fab region to freely interact with antigens. The soluble expression of recombinant protein proAx1-Au-binding in *E. coli* BL21(DE3) was achieved with 0.5 mM IPTG and an induction temperature of 37 °C for 4 hr. ProAx1-Au-binding was shown to bind better to AuNPs than proAx1 in pH 4.5 and the binding remained even after several cycles of washing, which is important when dealing with low-pH samples in immunoassays (Foley *et al.*, 2020; Isanga *et al.*, 2017). The improved gold-binding ability of protein A after being fused with a GBP is consistent with a previous publication in which protein A was also fused with another material-binding protein and thus displayed a higher affinity for that particular material compared to unmodified protein A (Tran-Nguyen *et al.*, 2021). This proves that protein A can be fused with different material-binding proteins/peptides to improve its binding capability to different materials (Faccio, 2018). Furthermore, other GBPs can be screened and genetically modified to obtain higher affinity to gold surfaces so that protein A-GBP fusion proteins could be immobilized even more effectively and stably onto AuNPs in different extreme conditions (Hnilova *et al.*, 2008).

The immobilization of antibodies via protein A-GBP fusion protein was shown to be more effective than other strategies, thus proving that the fusion with GBP did not affect the antibody-binding capability of protein A (Faccio,

2018). This novel strategy is expected to help orientate any antibody with affinity to protein A easily and stably toward the gold surface without chemical modification of antibodies (Jazayeri *et al.*, 2016). However, to guarantee the potential applications of protein A-GBP fusion protein in immunoassays and biosensors, the antigen-capture efficiency of this novel strategy would need to be further assessed.

5. Conclusion

In this work, a two-domain protein (proAx1-Au-binding) has been constructed to provide a new strategy for effective oriented immobilization of antibodies onto AuNPs. We successfully cloned the *proAx1-Au-binding* gene which encodes the two-domain protein proAx1-Au-binding. The gold-binding ability of proAx1-Au-binding was assessed and compared with a protein A domain (proAx1). ProAx1-Au-binding showed a higher binding capacity to AuNPs than proAx1 in pH 4.5. The strategy to immobilize antibodies onto AuNPs through proAx1-Au-binding also greatly improved the immobilizing efficiency compared to other conventional methods which were direct absorption and immobilizing via protein A. In conclusion, the results showed that the two-domain proAx1-Au-binding was a promising tool for the immobilization of antibodies onto the gold surface.

Acknowledgment

Thanh-Tan Nguyen was funded by the Master, PhD Scholarship Programme of Vingroup Innovation Foundation (VINIF), code VINIF.2022.ThS.077.

References

- Akbarzadeh Khiavi M, Safary A, Aghanejad A, Barar J, Rasta SH, Golchin A, Omidi Y and Somi MH. 2019. Enzyme-conjugated gold nanoparticles for combined enzyme and photothermal therapy of colon cancer cells. *Colloids Surf A: Physicochem Eng.*, **572**: 333-344.
- Al-Homsi L, Al-Assad J, Kweider M, Al-Okla S and Abbady AJJBS. 2012. Construction of pRSET-sfGFP plasmid for fusion-protein expression, purification and detection. *Jordan J Biol Sci.*, **5(4)**: 279-288.
- Bakshi S, He ZL and Harris WG. 2014. Natural Nanoparticles: Implications for Environment and Human Health. *Crit Rev Environ Sci Technol.*, **45(8)**: 861-904.
- Bhumkar DR, Joshi HM, Sastry M and Pokharkar VB. 2007. Chitosan Reduced Gold Nanoparticles as Novel Carriers for Transmucosal Delivery of Insulin. *Pharm Res.*, **24(8)**: 1415-1426.
- Deka J, Mojumdar A, Parris P, Onesti S and Casalis L. 2017. DNA-conjugated gold nanoparticles based colorimetric assay to assess helicase activity: a novel route to screen potential helicase inhibitors. *Sci Rep.*, **7(1)**.
- Dreaden EC, Alkilany AM, Huang X, Murphy CJ and El-Sayed MA. 2012. The golden age: gold nanoparticles for biomedicine. *Chem Soc Rev.*, **41(7)**: 2740-2779.
- Faccio G. 2018. From Protein Features to Sensing Surfaces. *Sensors*, **18(4)**: 1204.
- Foley MM, Brown CO, Westring CG, Danielson PB and McKiernan HE. 2020. Effects of organic acids and common household products on the occurrence of false positive test results

- using immunochromatographic assays. *Forensic Sci Int.*, **308**: 110165.
- Hnilova M, Oren EE, Seker UOS, Wilson BR, Collino S, Evans JS, Tamerler C and Sarikaya M. 2008. Effect of Molecular Conformations on the Adsorption Behavior of Gold-Binding Peptides. *Langmuir*, **24(21)**: 12440-12445.
- Isanga J, Tochi BN, Mukunzi D, Chen Y, Liu L, Kuang H and Xu C. 2017. Development of a specific monoclonal antibody assay and a rapid testing strip for the detection of apramycin residues in food samples. *Food Agric Immunol.*, **28(1)**: 49-66.
- Jans H, Liu X, Austin L, Maes G and Huo Q. 2009. Dynamic light scattering as a powerful tool for gold nanoparticle bioconjugation and biomolecular binding studies. *Anal Chem.*, **81(22)**: 9425-9432.
- Jansson B, Uhlén M and Nygren P-Å. 1998. All individual domains of staphylococcal protein A show Fab binding. *FEMS Immunol Med Microbiol.*, **20(1)**: 69-78.
- Jazayeri MH, Amani H, Pourfatollah AA, Pazoki-Toroudi H and Sedighimoghaddam B. 2016. Various methods of gold nanoparticles (GNPs) conjugation to antibodies. *Sens Biosensing Res.*, **9**: 17-22.
- Katz E and Willner I. 2004. Integrated nanoparticle-biomolecule hybrid systems: synthesis, properties, and applications. *Angew Chem Int Ed Engl.*, **43(45)**: 6042-6108.
- Ko S, Park TJ, Kim HS, Kim JH and Cho YJ. 2009. Directed self-assembly of gold binding polypeptide-protein A fusion proteins for development of gold nanoparticle-based SPR immunosensors. *Biosens Bioelectron.*, **24(8)**: 2592-2597.
- Kumari Y, Singh SK, Kumar R, Kumar B, Kaur G, Gulati M, Tewari D, Gowthamarajan K, Karri V, Ayinkamiye C, Khurshed R, Awasthi A, Pandey NK, Mohanta S, Gupta S, Corrie L, Patni P, Kumar R and Kumar R. 2020. Modified apple polysaccharide capped gold nanoparticles for oral delivery of insulin. *Int J Biol Macromol.*, **149**: 976-988.
- Le-Dao H-A, Le-Nguyen Y-V and Tran-Van HJJJoBS. 2022. Prokaryotic Expression of Murine Cellular Prion Protein for In vitro Evaluation. *Jordan J Biol Sci.*, **15(3)**.
- Lee H, Lee EM, Reginald SS and Chang IS. 2021. Peptide sequence-driven direct electron transfer properties and binding behaviors of gold-binding peptide-fused glucose dehydrogenase on electrode. *iScience*, **24(11)**: 103373.
- Lin X, O'Reilly Beringhs A and Lu X. 2021. Applications of Nanoparticle-Antibody Conjugates in Immunoassays and Tumor Imaging. *AAPS J.*, **23(2)**.
- Mohammad E and Soukkarieh CJJJoBS. 2022. A simple and cost Effectively Method for Production of Recombinant of Full Length of Human Placenta-Specific Protein using E. coli BL21 strain. *Jordan J Biol Sci.*, **15(5)**.
- Moks T, Abrahmsén L, Nilsson B, Hellman U, Sjöquist J and Uhlén M. 1986. Staphylococcal protein A consists of five IgG-binding domains. *Eur J Biochem.*, **156(3)**: 637-643.
- Nguyen TT, Vo-Nguyen HV and Tran-Van H. 2021. Prokaryotic expression of chimeric GFP-hFc protein as a potential immune-based tool. *Mol Biol Res Commun.*, **10(3)**: 105-108.
- Park TJ, Lee SY, Lee SJ, Park JP, Yang KS, Lee KB, Ko S, Park JB, Kim T, Kim SK, Shin YB, Chung BH, Ku SJ, Kim DH and Choi IS. 2006. Protein nanopatterns and biosensors using gold binding polypeptide as a fusion partner. *Anal Chem.*, **78(20)**: 7197-7205.
- Rahme K, Guo J and Holmes JD. 2019. Bioconjugated Gold Nanoparticles Enhance siRNA Delivery in Prostate Cancer Cells. *Methods Mol Biol.*, **1974**: 291-301.
- Saha B, Evers TH and Prins MW. 2014. How antibody surface coverage on nanoparticles determines the activity and kinetics of antigen capturing for biosensing. *Anal Chem.*, **86(16)**: 8158-8166.
- Thomas M and Klivanov AM. 2003. Conjugation to gold nanoparticles enhances polyethylenimine's transfer of plasmid DNA into mammalian cells. *Proc Natl Acad Sci U S A.*, **100(16)**: 9138-9143.
- Tran-Nguyen TS, Ngo-Luong DT, Nguyen-Phuoc KH, Tran TL and Tran-Van H. 2021. Simultaneously targeting nitrocellulose and antibody by a dual-headed protein. *Protein Expr Purif.*, **177**: 105764.
- Verde AV, Acres JM and Maranas JK. 2009. Investigating the Specificity of Peptide Adsorption on Gold Using Molecular Dynamics Simulations. *Biomacromolecules.*, **10(8)**: 2118-2128.